Flow Measurement and Instrumentation 51 (2016) 1–7

Contents lists available at ScienceDirect

Flow Measurement and Instrumentation

journal homepage: www.elsevier.com/locate/flowmeasinst

Support vector regression for modified oblique side weirs discharge coefficient prediction

Amir Hossein Zaji [a], Hossein Bonakdari [a], Shahaboddin Shamshirband [b,*]

[a] Department of Civil Engineering, Razi University, Kermanshah, Iran
[b] Department of Computer System, Faculty of Computer Science and Information Technology, University of Malaya, 50603 Kuala Lumpur, Malaysia

ARTICLE INFO

Article history:
Received 20 September 2015
Received in revised form
12 June 2016
Accepted 10 August 2016
Available online 11 August 2016

Keywords:
Discharge coefficient
Polynomial function
Radial basis function
Support vector regression
Triangular side weir

ABSTRACT

Accurate determination of discharge coefficient is one of the major concerns in the process of the designing of side weirs. Relation between the modified side weirs discharge coefficient to various geometric and hydraulic situations leads to a high flow complexity around the weirs. In this study, two types of support vector regression (SVR) methods were employed to model the discharge coefficient of a modified triangular side weir. Two types of SVR are obtained by using the radial basis and polynomial as the kernel functions. Six different non-dimensional input combinations with different input variables were used to find the most appropriate one. The results show that both SVR-rbf and SVR-poly methods perform better when the number of input variables is higher, and there is no compaction in the non-dimensional input variables. Comparison between the investigated models shows that the SVR-rbf by *RMSE* of 0.063 performs much better that SVR-poly by *RMSE* of 0.084.

1. Introduction

Side weirs are widely used in flow control structures such as irrigation and drainage, sewage, flood control and diversion systems. Side weirs are simple structures that set along the main channel side wall to control the flow rate and height. De Marchi [1] provided the first mathematical relations to calculate the discharge variation along the side weir (Eq. (1)).

$$-\frac{dQ}{dx}=\frac{2}{3}Cd\sqrt{2g}(y-w)^{1.5} \tag{1}$$

where Cd is the discharge coefficient, y depth of flow, w weir height, g gravity acceleration and dQ/dx discharge variation along the main channel. The primary assumption used to obtain this equation is the equality of the specific energy upstream and downstream of the side weir that was investigated and verified in other studies [2–4].

Primary side weirs have a rectangular shape. Rectangular side weirs are the simplest types of side weirs. There are various studies done on the discharge coefficient simulation of the rectangular channels [5–9].

There are two major alternatives to improve the diversion ability of the side weirs; increase the length of the side weir or increase the efficiency of the side weir. Increasing the side weir length requires the increase of the tributary width that seems costly. In addition, in cases where there is limitation in the tributary channel width, this alternative is impossible. One of the major tasks that can be performed to improve the side weir efficiency is to make some shape modification. Shape modification could increase the discharge coefficient of the side weir by 1.5–4.5 times compared to the traditional rectangular side weirs [10,11]. Various types of modified side weirs are such as triangular, labyrinth and elliptical ones. Various researches were done to determine the shape modified side weirs characteristics [11–19].

Because of the complexity of flow properties and the need to accurately predict the characteristics, soft computing methods are widely used in modeling the side weir characteristics. Bilhan et al. [20] used Feed Forward Neural Network (FFNN) and Radial Basis Neural Network (RBNN) methods to predict the discharge coefficient of a sharp-crested rectangular side weir located in a straight channel. Emiroglu et al. [21] predicted the discharge coefficient of triangular labyrinth side weirs by using adaptive neuro-fuzzy interface system (ANFIS) and found that ANFIS could significantly predict the discharge coefficient with more accuracy. Bilhan et al. [10] modeled the discharge coefficient of a triangular side weir that is located in a curved channel by using the Artificial Neural Network (ANN) method. The authors concluded that triangular side weirs are more efficient than traditional side weirs by up to 4.5 times. Dursun et al. [22] modeled the discharge coefficient of a semi-elliptical side weir by using ANFIS. The Authors concluded that ANFIS could successfully be used in discharge coefficient prediction, and it performs much better than Multiple Linear and

* Corresponding author.
E-mail address: shamshirband1396@gmail.com (S. Shamshirband).

http://dx.doi.org/10.1016/j.flowmeasinst.2016.08.006
0955-5986/© 2016 Elsevier Ltd. All rights reserved.

Nonlinear Regression methods (MLR and MNLR). Zaji and Bonakdari [23] compared the Multi-Layer Perceptron Neural Network (MLPNN), RBNN and Particle Swarm Optimization (PSO) based equations to predict the discharge coefficient of a modified triangular side weir. The authors found that the RBNN could predict the discharge coefficient of modified triangular side weirs with the highest accuracy amongst the three methods.

The aim of this study is to predict the discharge coefficient of a modified triangular side weir. Discharge coefficient of these side weirs were dependent on various variables such as weir length (L), weir height (w), weir included angle (θ), main channel width (b), upstream Froude number (Fr_1) and upstream flow depth (y_1). Because of the complex nature and multivariable dependency, a high-performance soft computing is needed to model the discharge coefficient of modified side weirs. Support vector regression (SVR) is employed in this study to modeling the discharge coefficient. To find the appropriated SVR, two methods were examined. The first one, the SVR-rbf uses radial basis function as the kernel function and the second one, the SVR-poly uses the polynomial kernel function. Six different non-dimensional input combinations were performed and tested with the SVR-rbf and SVR-poly methods to determine the most useful input variables. To train and test the SVR methods, the experimental dataset of Borghei and Parvaneh [11] were used.

2. Experimental dataset

The experimental study of Borghei and Parvaneh [11] were used to train and test the SVR-rbf and SVR-poly methods. The authors introduced a modified triangular side weir that performs up to about two times more efficient than the traditional side weirs (Fig. 1).

The main channel has a horizontal bed, 0.4 m width, and 11 m length. Glass made side walls with a height of 0.66 m were used. The experiments were done in various geometry and hydraulic situations by varying the weir length (L) between 0.3 m to 0.6 m, weir height between 50 mm to 150 mm, weir included angle (θ) between 60° to 140°, upstream Froude number (Fr_1) between 0.19 to 0.96 and upstream flow depth between 0.08 m to 0.2 m. The variation of the parameters in each experiment is shown in Table 1.

In the experimental study, two hundred measurements were done in various hydraulic and geometric situations. The accuracy of head measurements was ± 1 mm, and the accuracy of the discharge measurements was ± 0.0001 m^3/s.

3. Material and methods

3.1. Input parameters

As with other soft computing methods, the prediction accuracy of the SVR models is directly dependent on the selection of the appropriate input combination. In this study, comprehensive input combinations were examined to find the appropriate one. Table 2 shows the six different input combination that were investigated as the input variables of the SVR-rbf and SVR-poly.

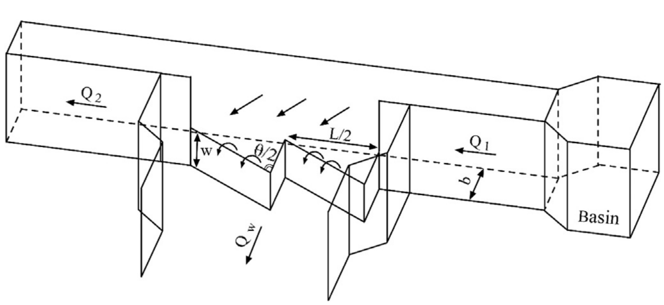

Fig. 1. Modified labyrinth side weir [11].

Table 1
The different geometric and hydraulic parameters used for the modified labyrinth side weir Borghei, Parvaneh [11].

$\theta/2$ (deg)	L (m)	w (mm)	w/y_1	Q_1 (m^3/s)	Fr_1	Number of runs
30	0.3	50,75,100,150	0.46–0.83	0.019–0.030	0.19–0.96	40
	0.4	50,75,100,150				
45	0.3	50,75,100,150	0.46–0.83	0.019–0.030	0.19–0.96	55
	0.4	50,75,100,150				
	0.6	50,100,150				
60	0.3	50,75,100,150	0.46–0.83	0.019–0.030	0.19–0.96	50
	0.4	50, 100,150				
	0.6	50, 100,150				
70	0.3	50,75,100,150	0.46–0.83	0.019–0.030	0.19–0.96	55
	0.4	50,75,100,150				
	0.6	50,100,150				

Table 2
Different examined input combinations.

Input name	Input variables
Input#1	w/b, y_1/b, L/b, $\sin(\theta/2)$, Fr_1
Input#2	w/y_1, L/b, $\sin(\theta/2)$, Fr_1
Input#3	w/y_1, $L\sin(\theta/2)/b$, Fr_1
Input#4	$w\ Fr_1/y_1$, L/b, $\sin(\theta/2)$
Input#5	wL/by_1, $Fr_1\sin(\theta/2)$
Input#6	$wLFr_1\sin(\theta/2)/by_1$

Some soft computing methods perform better when the number of the input variable is low, and adversely, some others perform better when the number input variables is high. In Table 2, it could be seen that the input variables of each input combination is different. The first input combination uses five no-compact input variables of w/b, y_1/b, L/b, $\sin(\theta/2)$, Fr_1 and the last input combination uses one compact input variable of $wLFr_1\sin(\theta/2)/by_1$.

The input variables of the input combination consist of non-dimensional combinations of the geometric (w, b, L and θ) and hydraulic (Fr_1 and y_1) conditions. The statistical properties of the non-dimensional variables are provided in Table 3. The standard deviation showed the distribution of the samples around the mean value and presented the degree of consistency among the samples of each variable.

Table 3
Statistical parameters of modified triangular discharge coefficient.

Variables	Statistical parameters			
	Min	Max	Mean	Standard deviation
w/b	0.125	0.375	0.241	0.095
y_1/b	0.200	0.513	0.348	0.096
L/b	0.750	1.500	1.010	0.290
w/y_1	0.461	0.831	0.671	0.098
$\sin(\theta/2)$	0.499	0.939	0.769	0.161
Fr_1	0.192	1.001	0.438	0.181
$L\sin(\theta/2)/b$	0.374	1.409	0.788	0.304
$w\ Fr_1/y_1$	0.134	0.607	0.281	0.091
wL/by_1	0.352	1.247	0.679	0.220
$Fr_1\sin(\theta/2)$	0.112	0.816	0.334	0.152
$wLFr_1\sin(\theta/2)/by_1$	0.067	0.593	0.219	0.108